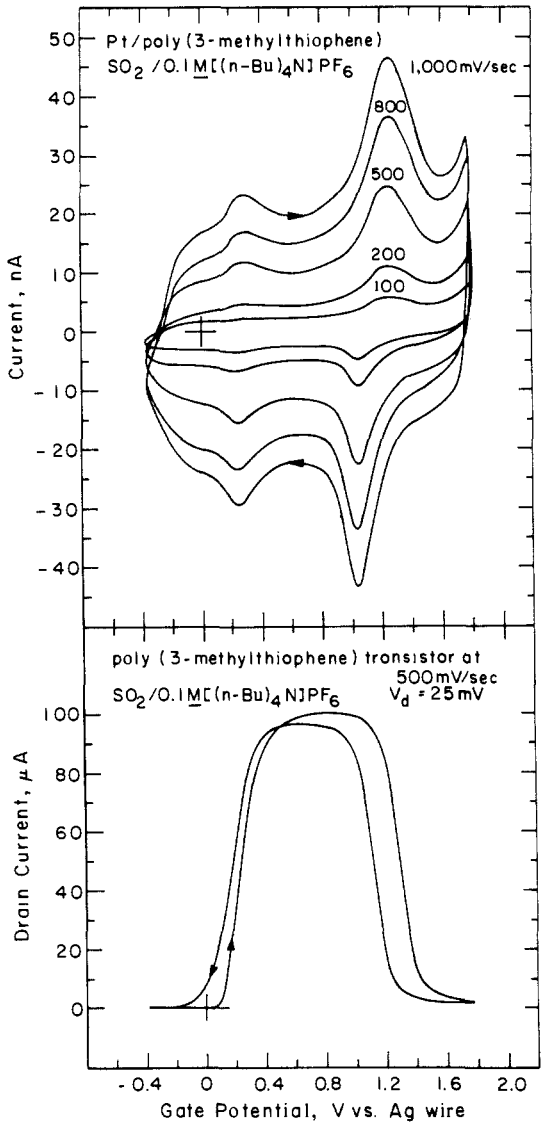

Figure 1. Top: Scan rate dependence for cyclic voltammetry of I on three adjacent Pt microelectrodes in SO_2/0.1 M $[(n\text{-}Bu)_4N]PF_6$. Bottom: I_D–V_G characteristic for an adjacent pair of the microelectrodes coated with I for which cyclic voltammetry is shown. In the region of maximum I_D, the current is partially limited by the significant resistance of the microelectrode leads (~200 Ω). All data are for solutions at −40 °C.

Figure 1 also shows the I_D–V_G characteristic in liquid SO_2/0.1 M $[(n\text{-}Bu)_4N]PF_6$ at −40 °C for an adjacent pair of Pt microelectrodes connected with I. Negative of 0.6 V versus Ag, the I_D–V_G characteristic corresponds to that previously observed in both liquid and solid electrolyte systems.[3,11] The new finding is that the conductivity of I significantly declines as the polymer is further oxidized, as reflected in the small values of I_D at very positive values of V_G. The polymer resistances at −0.2, +0.9, and +2.0 V versus Ag are $>10^{10}$ Ω, <100 Ω, and $\sim 10^4$ Ω, respectively. The region of high conductivity is ~1.3 V, much wider than for polyaniline.[5,6] The hysteresis evident in the I_D–V_G curve is scan rate independent in the range 10^1–10^3 mV/s and correlates with hysteresis in the cyclic voltammetry. Hysteresis in the properties of conducting polymers upon redox cycling has been explained as resulting from changes in polymer structure.[12] The behavior of II made by anodic polymerization of 2,2′-bithiophene on Pt microelectrodes is very similar to that of I, except that the region of high conductivity is more narrow (~1.0 V width), and the maximum conductivity is somewhat less.

The observation of lowered conductivity in highly oxidized polythiophenes is consistent with theoretical expectations[1,8] and is similar to observations made for polyaniline.[5,6] Considering the data for polyaniline,[5,6] I, and II, it does appear that the polymer with the greatest conductivity, I, also has the widest region of conductivity. Earlier, studies of the potential dependence of the conductivity of polypyrrole have been reported for a limited potential range.[9,13] We are currently investigating polypyrrole and its derivatives over a wider potential range to determine the width of the region of conductivity in these cases. Our findings have important practical implications relating to the use of conducting polymers I and II as electronic materials in batteries and microelectronic devices, since the polymers are shown to have a finite potential window where high conductivity occurs.

Acknowledgment. We thank the Office of Naval Research, the Defense Advanced Research Projects Agency, and the National Science Foundation through the M.I.T. Materials Research Laboratory for partial support of this research. We thank Professor R. J. Silbey for several valuable discussions.

(11) Chao, S.; Wrighton, M. S. *J. Am. Chem. Soc.* **1987**, *109*, 2197.
(12) (a) Kaufman, J. H.; Kaufer, J. W.; Heeger, A. J.; Kaner, R.; MacDiarmid, A. G. *Phys. Rev. B* **1982**, *26*, 2327. (b) Chung, T.-C.; Kaufman, J. H.; Heeger, A. J.; Wudl, F. *Phys. Rev. B* **1984**, *30*, 702.
(13) Feldman, B. J.; Burgmayer, P.; Murray, R. W. *J. Am. Chem. Soc.* **1985**, *107*, 872.

Studies of Phosphorylated Sites in Proteins Using ^1H–^{31}P Two-Dimensional NMR: Further Evidence for a Phosphodiester Link between a Seryl and a Threonyl Residue in *Azotobacter* Flavodoxin

David H. Live*,† and Dale E. Edmondson‡

Departments of Chemistry and Biochemistry
Emory University, Atlanta, Georgia 30322
Received January 25, 1988

Elucidation of sites of phosphorylation in proteins is important because of the significant effects of this modification on protein function. Current approaches to identify sites of phosphorylation use degradative chemical methods, which may not be satisfactory due to possible migration of the phosphate group. Direct ^{31}P NMR analysis provides little information on the identity of the amino acid residue phosphorylated since the shift value of the resonance can be influenced by a variety of factors. We report here the application of proton-detected ^1H–^{31}P multiquantum 2-dimensional NMR in the direct determination of the sites of phosphorylation in a protein. The use of these 2D techniques in proteins for ^{15}N and ^{13}C correlations (where large one-bond coupling interactions exist) is now established and has been recently reviewed.[1] Not only can this 2D technique offer sensitivity enhancement over the heteronuclear detected 2D analogue, but it also provides the greatest spectral resolution in the ^1H dimension where it is needed most. Small long-range couplings have been used to mediate 2D spectra of protons with other nuclei in metalloproteins[2-4] and oligonucleotides ($M_r \leq 10$ kDa).[5-7]

In this study we have examined *Azotobacter* flavodoxin, a protein of about 20 kDa that is an electron carrier in the bacterial nitrogen fixation system.[8,9] ^{31}P NMR studies have resolved two signals, one from a covalently bound ^{31}P and a second from the

† Department of Chemistry.
‡ Department of Biochemistry.
(1) Griffey, R. H.; Redfield, A. G. *Q. Rev. Biophys.* **1987**, *19*, 51.
(2) Live, D. H.; Armitage, I. M.; Dalgarno, D. C.; Cowburn, D. *J. Am. Chem. Soc.* **1985**, *107*, 1775.
(3) Live, D. H.; Kojiro, D. L.; Cowburn, D.; Markley, J. L. *J. Am. Chem. Soc.* **1985**, *107*, 3043.
(4) Frey, M. H.; Wagner, G.; Vasak, M.; Sorensen, O. W.; Neuhaus, D.; Worgotter, E.; Kagi, J. H. R.; Ernst, R.; Wuthrich, K. *J. Am. Chem. Soc.* **1985**, *107*, 6847.
(5) Sklenar, V.; Miyashiro, H.; Zon, G.; Miles, H. T.; Bax, A. *FEBS Lett.* **1986**, *208*, 94.
(6) Byrd, R. A.; Summers, M.; Zon, G.; Fouts, C. S.; Marzilli, L. *J. Am. Chem. Soc.* **1986**, *108*, 504.
(7) Sklenar, V.; Bax, A. *J. Am. Chem. Soc.* **1987**, *109*, 7525.

0002-7863/88/1510-4468$01.50/0

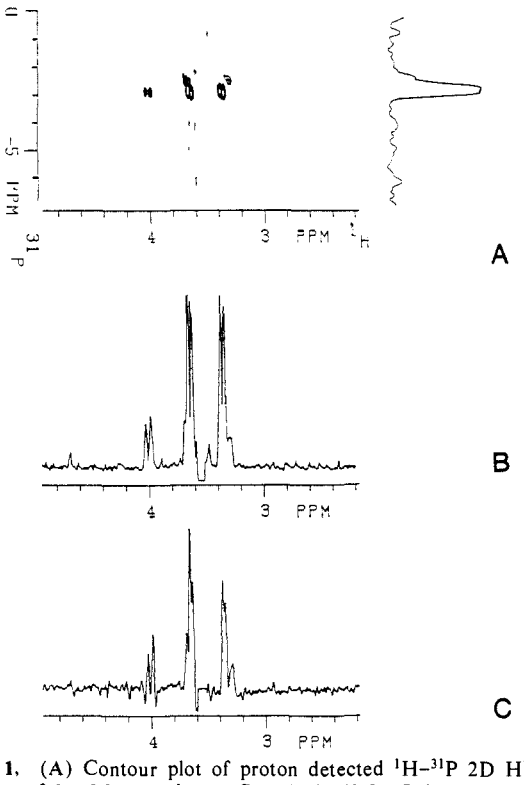

Figure 1. (A) Contour plot of proton detected ^1H–^{31}P 2D HMQC spectrum of 3 mM *Azotobacter* flavodoxin (0.5 mL in 5-mm sample tube) in D_2O with 50 mM Tris buffer at pH 8 presented in absolute value mode; 64 blocks of data (2048 scans each) were collected, with a recycle rate of 0.4 s. The t_1 (^{31}P) dimension was zero-filled twice to 256 points/2000 Hz. Digital resolution in the t_2 dimension was 512 points/2000 Hz. Unshifted sine bell filtering was applied in both dimensions. The ^{31}P projection is to the right. Shifts in the ^{31}P dimension are relative to aqueous trimethylphosphate, and shifts in the proton dimension are relative to TMS based on H_2O at 4.7 ppm. The pulse sequence used was $90(^1H)$–D–$90(^{31}P)$–$t_1/2$–$180(^1H)$–$t_1/2$–$90(^{31}P)$–acquire with phase cycling as reported in ref 15. D was set at 50 ms. Spectra were obtained on an NT-360 spectrometer (360 MHz ^1H, 146 MHz ^{31}P) modified so the decoupler could be used as a broad-band transmitter. A proton observe/broad-band decouple probe from Cryomagnet Systems, Inc. was used. (B) Proton projection of the 2D spectrum in A. (C) ^1H–^{31}P selective echo difference[12] spectrum of the same protein sample with time of 50 ms between the $90(^1H)$ and $180(^1H)$ pulses. Digital resolution was 4096 points/2000 Hz. Recycle time was 1.25 s. Scans (6144) were averaged, and a digital filtering (DM = 4) was used. Phase-sensitive data are presented. Some differences are evident between this spectrum and the projection in 1B since one is a magnitude spectrum while the other is phased and because of the different digital filtering and resolution.

phosphorylated flavin mononucleotide (FMN) coenzyme.[10,11] Comparison of ^1H coupled and decoupled ^{31}P spectra indicate coupling on the order of 10 Hz to the protein-bound phosphate and much smaller coupling to the FMN phosphate. Degradative chemical methods, although not unequivocal, have suggested that one seryl and one threonyl residue per protein are linked to a phosphate group. This finding, along with the 1D ^{31}P NMR data, suggest an unusual disubstituted phosphate residue that links a seryl to a threonyl residue;[10,11] however, further confirmation is needed for this unusual linkage. The 2D HMQC NMR results reported here on intact protein gives direct support for the existence of such a link. The 2D spectrum (Figure 1A) shows cross peaks only between protons and the phosphorus resonanting at the position of the protein-bound covalent phosphate. The pattern of the major peaks at 3.4 and 3.7 ppm in the proton projection (Figure 1B) and examination of the coupling constants shows that this phosphorus is coupled to two geminal protons of an AB type. This spectral pattern is seen independently in a $^1H(^{31}P)$ selective echo difference spectrum.[12] (This spectrum only reveals protons coupled to any phosphorus, not necessarily coupled to the same phosphorus.) These spectra can be obtained in a protein of this size even though the ^1H–^{31}P coupling is on the order of 10 Hz or less. The weaker cross peaks that correlate with a slightly downfield ^{31}P shift are due to a small amount of denaturated protein in the sample. Of the amino acids known to be phosphorylated in proteins, only protons from serine and threonine would have resonances in this shift range[13] and only the β protons of serine would give such an AB pattern. There is a weaker doublet in the proton dimension about 4.0 ppm downfield whose structure is seen clearly in Figure 1C. This is assigned to the α proton of a threonyl residue. This pattern is inconsistent with the higher multiplicity expected of the α protons in a phosphoseryl residue (due to coupling with two β protons). It is unlikely to be a signal from another phosphoseryl β proton since we did not see evidence for signal from the second β proton of a putative second phosphoserine. The only other residue that would have resonances in this region and that could be phosphorylated is a threonine. This signal could not, however, be a phosphothreonyl β proton since this proton resonance would consist of a doublet of quartets from couplings to α proton and γ methyl protons and might be further split by any phosphorus coupling. Thus, by elimination, the doublet at 4 ppm is attributed to a phosphothreonyl α proton. The absence of a signal from a phosphothreonyl β proton can be rationalized in terms of the reduction in peak height arising from the multiple couplings and the consequence of these couplings in the 2D experiment, where they can give rise to higher order multiquantum coherences, which do not revert to a detectable signal. Precedent for observing a strong cross peak for the α proton of phosphothreonine while not observing a significant one for the α of phosphoserine is found in control HMQC 2D experiments on these phosphorylated amino acids under the same spectral conditions as used for the protein. Spectra taken at pH 2 show the most intense correlation is between the α proton and the phosphorus in threonine. A 2D spectrum of phosphoserine, on the other hand, showed the most intense correlation to the β protons with virtually no intensity in the cross peak between the α proton and the phosphorus. Steric considerations would suggest that the added bulk of substituents on the β carbon of threonine would favor a situation where the dihedral angle between the ^{31}P and the β ^1H would approach zero, as would the heteronuclear coupling constant.

We have also successfully carried out this experiment on ovalbumin, a 43-kDa protein with two phosphoserines,[14] and find cross peaks to both phospho groups present. The appearance of the cross peaks is more similar to the free phosphoserine model than to our flavoprotein spectra. This supports our analysis of an unusual diester linkage in the latter protein.

In free FMN, the 5′ methylene protons exhibit cross peaks in a ^1H–^{31}P 2D spectrum. The protons coupled to the tightly bound FMN moiety in the protein are not observed. The lack of cross peaks to the protein-bound FMN could arise from H–C–O–P dihedral angles that result in weak couplings (indicated in the 1D ^{31}P experiments mentioned above) or from unfavorable relaxation and motional properties.

This work presents a novel approach to the characterization of the sites of covalent phosphate attachment in moderately sized proteins. This should extend to phosphorylated tyrosyl residues

(8) Tanaka, M.; Haniu, M.; Yasunobu, K. T.; Yoch, D. C. *Biochemistry* **1977**, *16*, 3525.
(9) The flavodoxin used in this work did not contain the "labile" phosphorus residue that was present in preparations used in ref 10 and 11.
(10) Edmondson, D. E.; James, T. L. *Proc. Nat. Acad. Sci., U.S.A.* **1979**, *76*, 3768.
(11) Edmondson, D. E.; James, T. L. In *Flavins and Flavoproteins*; Massey, V., Williams, C. H., Eds., Elsivier North Holland: Amsterdam, 1982; p 111.
(12) Cohen, J. S.; Chen, C.-W.; Bax, A. *J. Magn. Reson.* **1984**, *59*, 181.
(13) Other possible phosphorylated amino acids in proteins such as tyrosine, histidine, glutamate, or aspartate can be ruled out on the basis of their known chemical and NMR properties, which are not exhibited by the phosphorylated residues in this protein.
(14) Vogel, H. J.; Bridger, W. A. *Biochemistry* **1982**, *21*, 5825.
(15) Bax, A.; Griffey, R. H.; Hawkins, B. L. *J. Magn. Reson.* **1983**, *55*, 301.

since $^1H-^{31}P$ cross peaks arising from the four-bond coupling between the phosphorus and the ortho protons have been readily observed by us for the free amino acid.

Acknowledgment. This work was supported by NSF Grants DMB-8616952 and DMB-86061304. The NT-360 spectrometer was purchased with funds from the NSF and Emory University. Funds for implementation of indirect detection experiments were provided by the Emory University Research Fund.

Supplementary Material Available: Figures 1 and 2 containing proton projections of 2D $^1H-^{31}P$ HMQC data for 0.12 M phosphothreonine and 0.1 M phosphoserine in D_2O, respectively (3 pages). Ordering information is given on any current masthead page.

Cationic Oligonucleotides

Robert L. Letsinger,* Charles N. Singman, Gary Histand, and Manikrao Salunkhe†

Department of Chemistry, Northwestern University Evanston, Illinois 60208

Received March 29, 1988

The reversible association of oligonucleotides with complementary sequences is of basic importance in biotechnology. With the objective of gaining further understanding and control of hybridization we have synthesized and examined oligonucleotide analogues **1**, **2**, and **3**, which in neutral or acidic solution carry positive charges along the backbone. We present evidence here that these novel analogues bind to complementary oligonucleotides and show that the extent of interaction can be tuned selectively by changes in salt concentration and pH. Under appropriate conditions the cationic probes bind more effectively than their natural counterparts to single stranded polydeoxyribonucleotide sequences.

d(T+T+T+T+T+T+T+T+T+T+T+T) d(T-T+T-T+T-T+T-T+T)

1 **2**

d(TxTxCxTxGxAxAxAxAxT)

3

d(TTCTGAAAAT) d(ATTTTCAGAATTGGG)

3a **4**

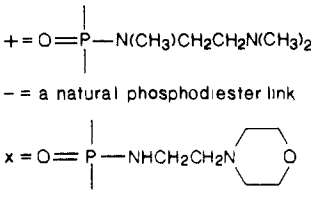

The oligomers were synthesized[1] on solid supports in syringes[2] or a Biosearch 8600 DNA synthesizer. Pertinent characterization data are given in Table I. Hydrolysis of **1** and **2** with 88% aqueous formic acid (95° 30 min) afforded dT_{10} and dT_9, respectively. Oligomers **1**, **2**, **3** were resistant to snake venom phosphodiesterase, spleen phosphodiesterase, and P1 nuclease.

Hybridization was assayed by changes in A_{260} as a function of temperature. As shown in Figure 1, the absorbance of a solution of **1** and polydA in 0.1 M NaCl at 0 °C is strongly reduced relative to that calculated for non-interacting oligomers. This hypochromic effect and the "melting out" on heating are indicative of a complex with ordered stacking of the bases. In 1.0 M NaCl the complex is relatively unstable. This response to changes in salt concentration is the reverse of that found for conventional nucleotide duplexes and is consistent with expectation for a complex stabilized by attraction of oppositely charged ions. Comparable experiments with **1** + polydT and **1** + polyrA served as useful negative controls. Essentially no hypochromic effect was observed, suggesting that specific hydrogen bonding is needed as well as ionic attraction and that bulky substituents at phosphorus interfere in formation

Table I. Properties of Oligonucleotides

compd	HPLC, elution time, (min)[a]	PAGE[b] Rm	^{31}P NMR[c]
1	8.2[d]	+1.2	+11.05
2	19.0	0	+10.37; -0.81
3	21.5	+0.90;[b] +0.1[e]	+10.7
dT_{10}	13.6	-0.86	
dT_9	13.6	-0.90	
3a	11.7	-0.87	

[a] Hewlett Packard RP-C18 column (10 cm) (except for **1**, see *d*); 0.1 M Et_3NHOAc (pH 7.0), 1%/min MeCN gradient starting at 0% MeCN; 0.5 mL/min flow rate. [b] Polyacrylamide gel electrophoresis; + indicates migration toward anode in 12% cross-linked gel, pH 5.0; Rm is distance relative to methylene blue; - indicates migration toward cathode in 20% cross-linked gel, pH 8.0, relative to bromophenol blue. [c] ppm relative to 85% H_3PO_4; + is downfield; D_2O solvent. [d] Beckman RPSC C-3 column (5 cm); 0.1 M Et_3NHOAc buffer, pH 5.6; 1%/min MeCN gradient starting at 5% MeCN; 1 mL/min flow rate. [e] pH 7.0.

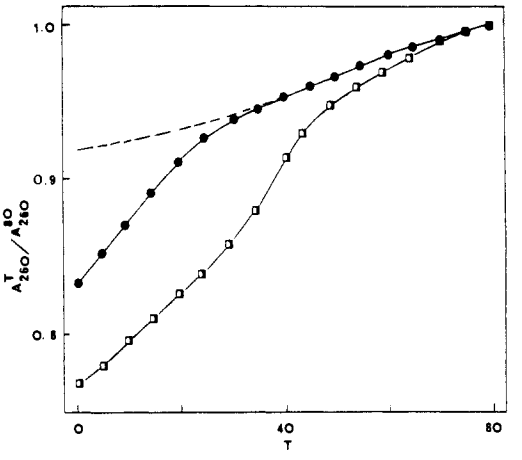

Figure 1. Absorbance profile at pH 7.1 (0.01 M Tris buffer): **1** + polydA (2T/dA) in 1 M NaCl (●), 0.1 M NaCl (□); calculated for **1** + polydA (2T/dA) from heating curves of separated samples of **1** and polydA, assuming no interaction of the oligomers (---).

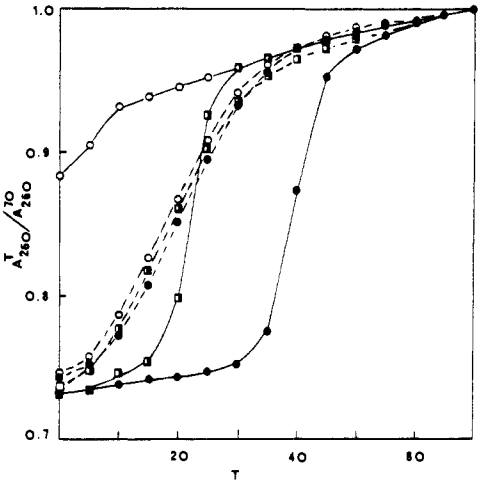

Figure 2. Absorbance profile at pH 7.0 (0.01 M Tris buffer): **2** + polydA (2T/dA) in 1.0 M NaCl (--●--), 0.1 M NaCl (--□--), no NaCl (--○--); dT_9 + polydA (2T/dA) in 1.0 M NaCl (-●-), 0.1 M NaCl (-□-), no NaCl (-○-).

† On study leave from the Department of Chemistry, Shivaji University, Kolhapur 416004, India.

(1) Methyl phosphoramidite chemistry[3] was used in generating phosphodiester links and hydrogen phosphonate chemistry[4] followed by oxidative coupling[5] with the appropriate diamine was used in generating the aminoalkylphosphoramidate links. Standard deprotection conditions were employed.

(2) Tanaka, T.; Letsinger, R. L. *Nucl. Acids Res.* **1982**, *10*, 3249-3260.

0002-7863/88/1510-4470$01.50/0